Magnetic Resonance in Medicine 62:1080–1084 (2009)

Experimental Protocol for Activation-Induced Manganese-Enhanced MRI (AIM-MRI) Based on Quantitative Determination of Mn Content in Rat Brain by Fast T_1 Mapping

S. Tambalo,[1] A. Daducci,[1] S. Fiorini,[1] F. Boschi,[1] M. Mariani,[2] M. Marinone,[3] A. Sbarbati,[1] and P. Marzola[1*]

In activation-induced manganese-enhanced MRI (AIM-MRI) experiments, differential accumulation of Mn in activated and silent brain areas is generally assessed using T_1-weighted images and quantified by the enhancement of signal intensity (SI), calculated with reference to SI before Mn administration or to SI of brain regions unaffected by the specific stimulus. However, SI enhancement can be unreliable when animals are removed from and reinserted into the magnet. We have developed an experimental protocol based on repeated intraperitoneal (i.p.) injections of Mn, quantitative determination of T_1, and coregistration of images to a rat brain atlas that allows absolute quantification of Mn concentration in selected brain areas. Results showed that interanimal variability of postcontrast T_1 values was very low (compared to the experimental error in T_1 determinations) allowing detection of differential regional Mn uptake in stimulated and unstimulated animals. In addition we have determined in vivo relaxivity of Mn in brain tissue and its frequency dependence. Magn Reson Med 62:1080–1084, 2009.

Key words: AIM-MRI; MEMRI; Mn; fMRI; brain

Manganese-enhanced MRI (MEMRI) is a relatively new method for investigation of neuronal pathways, enhancement of brain neuroarchitecture and functional MRI (fMRI) in laboratory animals (1,2). On the basis of Mn ions' capacity to enter excitable cells via voltage-gated calcium channels, MRI protocols have been devised that enable accumulation of Mn in active areas of the brain; this application has been termed activation-induced MEMRI (AIM-MRI) (1). Accumulation of Mn in specific brain areas can easily be monitored by MRI thanks to its effect on longitudinal relaxation time. Compared to standard blood oxygenation level dependent (BOLD) fMRI techniques, AIM-MRI has several advantages: 1) higher sensitivity and signal-to-noise ratio, which allows fMRI at high spatial resolution and/or with mild sensory stimulation (2); 2) unlike BOLD, AIM-MRI depends not on blood hemodynamics but directly on neuron activity; 3) Mn accumulation is visible in standard T_1-weighted images that are superior in terms of anatomical detail to T_2^*-weighted images used in BOLD acquisitions.

AIM-MRI experiments encompass three steps: 1) a certain amount of Mn ions needs to be delivered to the brain parenchyma; 2) the stimulus has to be applied; 3) differential accumulation of Mn in activated brain regions needs to be detected by T_1-weighted MRI. The first step has been performed using different modalities: intravenous (i.v.) injection (with or without artificial opening of the blood-brain barrier [BBB]), intracerebral, intraperitoneal (i.p.), or subcutaneous injection. Most of the AIM-MRI experiments reported in the literature have been performed after i.v. infusion of $MnCl_2$ and artificial opening of the BBB (2,3). However, some recent works have reported functional experiments performed after i.v. administration without BBB opening, or i.p. administration (4,5). Kuo et al. (4) reported detection of hypothalamic neuronal activity in vivo after i.v. administration of $MnCl_2$ without compromise of the BBB. Yu et al. (5) demonstrated that AIM-MRI can detect sound-evoked activity in awake mice behaving normally after i.p. administration of $MnCl_2$. I.p. infusion appears particularly interesting because it can be used to study functional response in awake animals, if MRI is performed after the presumed activity has occurred and is preceded by an i.p. injection of Mn (6).

Differential accumulation of Mn in activated and silent brain areas is generally assessed using standard T_1-weighted images and quantified by the enhancement of the signal intensity (SI), which is calculated with reference to the SI before Mn administration or to the SI of brain regions that are known to be unaffected by the specific stimulus. However, SI enhancement can be unreliable when animals are removed from and reinserted into the magnet, as protocols on awake animals require, or when nonactivated areas are not known a priori. Absolute determination of Mn concentration in specific brain areas appears to be a good alternative. Mn concentration can be absolutely quantified by measuring the tissue longitudinal relaxation time through the well-known correlation between the enhancement in the relaxation rate (ΔR_1) and Mn concentration (c): $\Delta R_1 = r_1 * c$, r_1 being the longitudinal

[1]Department of Morphological and Biomedical Sciences, University of Verona, Verona, Italy.

[2]Department of Physics "A. Volta", Consiglio Nazionale Interuniversitario per le Scienze fisiche della Materia (CNISM) and Consiglio Nazionale delle Ricerche (CNR)-Instituto Nazionale per la Fisica della Materia (INFM), University of Pavia, Pavia, Italy.

[3]Institute of Physiology and Biochemistry "G. Esposito," University of Milan, Milan, Italy.

Grant sponsor: European Center for Sustainable Impact of Nanotechnology (ECSIN), Rovigo, Italy.

Preliminary report given as an oral presentation at the Joint Annual Meeting ISMRM-ESMRMB, Berlin, Germany, 19–25 May, 2007.

*Correspondence to: Pasquina Marzola, Department of Morphological and Biomedical Sciences, Section of Anatomy, Strada Le Grazie 8, I-37134 Verona, Italy. E-mail: pasquina.marzola@univr.it

Received 28 October 2008; revised 17 February 2009; accepted 29 April 2009.

DOI 10.1002/mrm.22095

Published online 1 September 2009 in Wiley InterScience (www.interscience.wiley.com).

relaxation of Mn in the brain. In this study we implemented an MRI protocol based on fast T_1 mapping and coregistration to rat brain atlas, which made possible absolute quantification of Mn concentration in different brain regions. The aim of the study was to implement an MRI protocol based on quantitative Mn determination, to be used in AIM-MRI experiments.

MATERIALS AND METHODS

Animals and MRI Experiments

Manganese solutions were prepared by dissolving 5.34 g of $MnCl_2$ (tetra hydrate; Sigma-Aldrich, Italy) in 100 ml of bicine buffer (Sigma-Aldrich) to obtain a final Mn concentration of 270 mM. These Mn solutions were administered i.p. to animals at a dose of 0.2 mmol/kg body weight. Twenty-eight male Sprague-Dawley rats (215 ± 23 g; Harlan, Italy) were used, subdivided into two groups: the first group of animals ($N = 8$) received three Mn injections at a dose of 0.2 mmol/kg over a period of 7 days (day 1, day 4, and day 7) and images were acquired on day 8; the second group of animals ($N = 10$) received two Mn injections at a dose of 0.2 mmol/kg over a 24-h period (day 1 and day 2) and images were acquired on day 3. Eight animals were used for the measurement of in vivo relaxivity. Two additional animals were used for determination of the frequency dependence of relaxation rate enhancement. All procedures were carried out following Italian regulations governing animal welfare and protection.

MRI experiments were carried out using a Biospec System (Bruker, Germany) equipped with a 4.7T, 33-cm bore horizontal magnet (Oxford, Ltd., UK), a 20-G/cm gradient insert, and an HP Linux RHE3 computer. A 72-mm birdcage volume coil and the Bruker quadrature "rat brain" coil were used for transmission and signal detection, respectively. After induction of anesthesia, in a preanesthesia box with a mixture of air and O_2 containing 5% of isoflurane (Forane; Abbott spa, Italy), rats were placed supine into the magnet and maintained with a mixture of air and oxygen containing 2% to 2.5% of isoflurane. T_1-weighted three-dimensional (3D) gradient-recalled echo (GRE) images were acquired to localize the olfactory bulb/anterior cortex endpoint, which was later used as a reference to set transversal acquisitions. Transversal multislice fast spin-echo T_2-weighted images (rapid acquisition with relaxation enhancement [RARE], $TE_{eff} = 70$ ms) were acquired and used to coregister images to the rat brain atlas (see Image Analysis section and Ref. 7). For T_1 measurement of the brain, a segmented inversion-recovery fast low-angle shot (IR-FLASH) sequence (8) was used, with TR = 10 ms, TE = 3.6 ms, matrix size = 128 × 128, field-of-view (FOV) = 3.5 × 3.5 cm^2, slice thickness = 1 mm, $\alpha = 5°$, inversion pulse = 5 ms hyperbolic secant (sech). The acquisition was divided into eight segments in the *k*-space in order to acquire at least three images before nulling of the signal (acquisition time = 160 ms per frame). Starting from the olfactory bulb/anterior cortex endpoint, 25 transversal slices were acquired. Ex vivo measurements of brain T_1 were performed at 37°C by using a Spinmaster (Stelar, Pavia, Italy) and an Apollo Spectrometer (Tecmag, Houston, TX, USA). The longitudinal spin-lattice relaxation time T_1 was measured through a standard saturation-recovery sequence.

Calibration of the T_1 Mapping Sequence and Determination of In Vitro and In Vivo Relaxivities

The T_1 mapping sequence was calibrated by correlating T_1 values obtained by imaging with values obtained by a standard spectroscopic sequence. Agarose gels (2%) containing different amounts of $MnCl_2$ (0.015, 0.03, 0.06, 0.125, 0.25, 0.5, and 1 mM) were prepared. For spectroscopic T_1 measurements, single gel phantoms were inserted into a 3.5-cm inner diameter (i.d.) birdcage coil; an IR sequence with two squared pulses (42 and 84 μs) was used; the inversion times ranged between 1/100 and five times the expected T_1 value. After the spectroscopic measurement, all the phantoms were inserted into a 7.2-cm i.d. birdcage coil for T_1 mapping using the IR-FLASH sequence. Images were acquired with the same parameters used in in vivo experiments. The relaxivity of Mn in agarose gel was obtained by least-squares linear fitting of the relaxation rate values of the gels as a function of Mn concentration. In vivo relaxivity was measured using $N = 8$ animals; T_1 maps of the whole brain were acquired before and 24 h after injection of 0.4 mmol/kg ($N = 2$), 0.3 mmol/kg ($N = 2$), or 0.2 mmol/kg ($N = 4$) of $MnCl_2$. The T_1 value was averaged over the whole brain. After the last acquisition the animals were sacrificed, the brains were removed, and Mn content was measured using atomic absorption spectroscopy (AAS). The frequency dependence of the relaxation rate enhancement was measured using two additional animals: one animal received 0.2 mmol/kg of Mn 24 h prior to sacrifice and the other received a similar volume of vehicle. Measurement of T_1 was performed on the excised brains in the frequency range between 1 and 55 MHz.

Image Analysis

Images were analyzed using Matlab R2007a (The MathWorks, Inc., Natick, MA, USA) and FSL 4.0 (FMRIB Group, University of Oxford, Oxford, UK). Parametric T_1 maps were calculated pixel-by-pixel by least-squares fitting according to Ref. 8. After denoising, in each pixel the theoretical expression of the SI:

$$SI(t) = A - B \cdot \exp(-t/T_1^*) \quad [1]$$

was fitted to experimental data. The true T_1 value was then calculated from the *effective* T_1* by

$$T_1 = T_1^* \cdot (B/A - 1). \quad [2]$$

Pixels in which T_1 values were longer than 3000 ms or shorter than 100 ms were excluded from the analysis. Coregistration of T_1 maps to the Paxinos and Watson brain atlas (9) was performed as described by Schwarz et al. (7), with some modifications. Briefly, acquired images were exported in the NIFTI-1 file-format; i.e., the standard file format adopted by FSL, which makes it possible to specify in the file header the orientation of images in the reference frame of the gradients. For each animal, T_2-weighted RARE

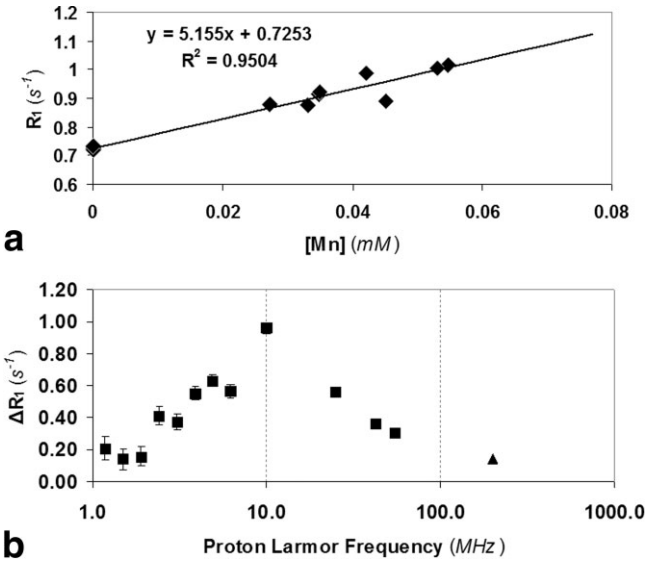

Figure 1. **a:** Average longitudinal relaxation rate of brain tissue as a function of Mn concentration; the slope of the best fitting line represents in vivo relaxivity of Mn ion (**b**) frequency dependence of the enhancement of brain relaxation rate, 24 h after administration of 0.2 mmol/kg of $MnCl_2$. Data in the range 1 to 55 MHz were measured ex vivo, while the value at 200 MHz was measured in vivo by imaging.

images were used for coregistration to the T_2-weighted template of the rat brain developed (7). For the alignment procedure, we used FSL FLIRT (10) software and a rigid 9 degrees of freedom (DOF) affine transformation. The normalized correlation was adopted as the cost function. The transformation matrix determined for the T_2-weighted scan was used to reorient all other acquisitions of the same subject. The T_2 template provided by Schwartz et al. (7) is coregistered to the Paxinos and Watson brain atlas (9) and consequently, after coregistration of scans to the template, we could extract regions of interest by querying structures from this brain atlas. Brain structures of interest were extracted from the atlas and superimposed over the T_1 maps of each subject. Average T_1 value in these regions, as well as in the whole brain, were calculated. Statistically significant differences were assessed by two-way analysis of variance (ANOVA) test for repeated measurements.

RESULTS

Mn Relaxivity In Vitro and In Vivo

The segmented IR-FLASH sequence was preliminarily tested by comparing the T_1 values obtained by imaging to those obtained by classical spectroscopic IR sequence in 2% agarose gels containing different amounts of $MnCl_2$. T_1 values determined by imaging were linearly correlated with those obtained by spectroscopy: $T_{1IM} = 0.9775 * T_{1SP} + 0.0358$, $R^2 = 0.997$. The relaxivity of Mn^{2+} in gel amounted to $r_1 = 3.74 \pm 0.60$ $mM^{-1}s^{-1}$ as measured by imaging, which was not different from the value obtained using spectroscopy, 3.54 ± 0.59 $mM^{-1}s^{-1}$. For in vivo relaxivity, the average brain T_1 relaxation times of animals before and 24 h after receiving $MnCl_2$, as well as the total Mn content, were determined. Results are shown in Fig. 1a, where Mn content is expressed in mM concentration, taking 1.041 mg/ml to be the average density of brain tissue (11). Mn relaxivity in the brain amounted to 5.15 ± 0.78 $mM^{-1}s^{-1}$, which was higher than in gels, possibly due to binding with proteins or other cellular components, but was substantially lower than data reported in the literature (2,12). The low value of relaxivity observed in the present study is attributable to the high frequency (200 MHz), since relaxivity data reported in the literature are generally acquired at 20 MHz (2,12). Figure 1b reports the frequency dependence of the relaxation rate enhancement in the rat brain 24 h after administration of Mn (0.2 mmol/kg), measured ex vivo in the range 1 to 55 MHz; the value at 200 MHz was obtained in vivo by imaging. A clear peak is observed at about 10 MHz and then the relaxation rate enhancement rapidly decreases: at 200 MHz, the relaxation rate is about 10 times lower than its maximum value.

Quantification of Mn in Different Brain Areas After Repeated Injections

Figure 2 shows representative 3D acquisitions of rat brain before and at different time points after i.p. administration of 0.2 mmol/kg $MnCl_2$. The animal was removed and reinserted into the magnet twice (for the 12-h and 24-h acquisitions) but coregistration of images allowed perfect spatial reproducibility of the slices. Figure 2 shows that within the first hour after administration, $MnCl_2$ enhanced brain regions without BBB, such as the choroid plexus and pituitary gland, in line with previously reported findings (13). At later time points, $MnCl_2$ started to diffuse into brain parenchyma and 24 h after administration, enhancement of the choroid plexus had almost disappeared, indicating diffusion from the ventricular space into brain tissue. Figure 3a reports T_1 values measured in different brain regions using two administration protocols; data are reported as mean $\pm$ SD over the experimental group. It is clearly apparent that interanimal variability of postcontrast T_1 values is very low (the SD in all the brain regions considered was between 3% and 8% of the T_1 value, i.e., of the order of experimental error in T_1 determinations). I.p.

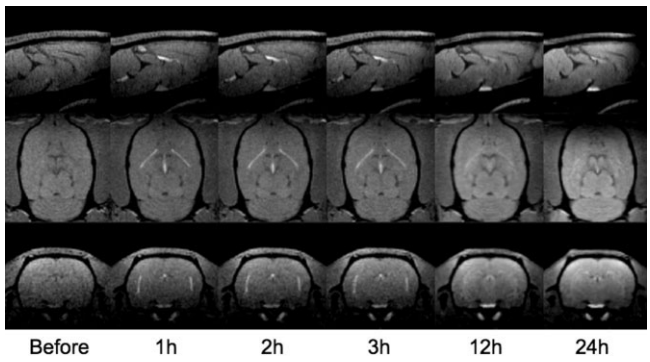

Figure 2. Transversal, coronal, and sagittal slices from 3D images acquired before and at different time points after administration of 0.2 mmol/kg of $MnCl_2$. The animal was removed and reinserted into the magnet for the 12 h and 24 h acquisition. Images were coregistered as described in the text.

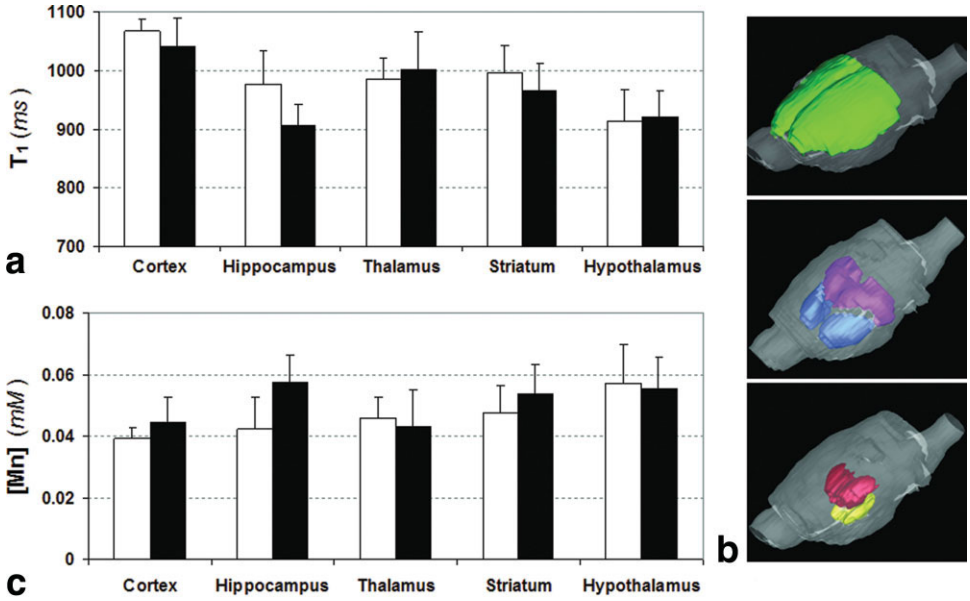

Figure 3. **a:** Postcontrast T_1 values measured in different brain regions after two (white bars) or three (black bars) injections of $MnCl_2$. **b:** Anatomical regions used for quantitative evaluations of relaxation times: the cortex in green, thalamus in red, hypothalamus in yellow, striatum in blue, hippocampus in pink. **d:** Concentration of Mn in different brain areas.

administration of a certain dosage of Mn delivers reproducible amounts of Mn to the brain. This finding is important for potential applications of this protocol in fMRI: interanimal reproducibility of Mn uptake should make it possible to detect differential regional uptake of Mn in stimulated and unstimulated animals. Postcontrast T_1 value averaged over the whole brain amounted to 968 $\pm$ 36 ms in the group receiving two Mn injections, which was not different from the average value in the group receiving three injections (966 $\pm$ 43 ms). Figure 3b shows the anatomical regions used for quantitative evaluations. The two administration protocols delivered similar amounts of Mn to different brain regions; postcontrast T_1 values were not statistically different (except in the hippocampus). Figure 3b reports quantitative concentration data obtained from measured T_1 brain values and Mn relaxivity. Mn concentration in the brain areas considered ranged between 0.04 and 0.06 mM.

DISCUSSION

There is rapidly increasing interest in MEMRI as a technique for functional and morphological imaging (14,15). In this work we propose an experimental algorithm based on fast T_1 mapping and coregistration of brain images to a rat brain atlas that allows absolute quantification of Mn concentration in selected brain areas, which in principle would allow experimental protocols in which a stimulus is applied to awake animals behaving normally. Compared to standard BOLD fMRI, MEMRI has several advantages. The most important are that it does not measure signals of vascular origin, but events directly related to cellular depolarization, and that thanks to its high in vivo longitudinal relaxivity, it allows detection of activation with high sensitivity. Relevant toxic effects have been reported for cumulative Mn dosages comparable to those used in the present investigation, although such effects were decreased by administration of fractionated dosages (16). Mn toxicity is indeed a big disadvantage of MEMRI techniques that is likely to limit their transferability to human studies. Development of Mn-based contrast agents, with slow release of Mn^{2+}, as well as of acquisition techniques sensitive to very small changes in water T_1 represent possible ways to develop MEMRI protocols suitable for human studies (17).

Here we measured in vivo Mn relaxivity in rat brain, obtaining a value substantially lower than those reported in the literature (2,12). The frequency dependence of brain relaxation rate enhancement induced by the presence of Mn clarifies the origin of this low value: relaxation rate enhancement shows a maximum at low fields, around 10 MHz, and then a typical decreasing trend, as observed when Mn ions are bound to proteins (18,19) or other cellular components. The above- mentioned value for in vivo relaxivity was used to estimate Mn concentration in different brain areas. With our experimental protocol, typical values for Mn concentrations were in the range 0.04 to 0.06 mM. It is worthwhile to mention that the above concentration values were calculated by using the mean relaxivity of Mn in brain, while the true Mn relaxivity could be dependent on its location and binding status. This approach may result with a not easily quantifiable degree of inaccuracy in calculated concentration values.

In this study we used a fast T_1 mapping technique to quantitatively determine the content of Mn in different brain areas using two administration protocols: three injections over a 7-day period and two injections over a 24-h period. In our experimental conditions we injected cumulative dosages of 0.6 and 0.4 mmol/kg of Mn, corresponding to about 120 and 80 mg/kg of $MnCl_2$-$4H_2O$. Surprisingly, our results show that the amount of Mn delivered to the whole brain or to different brain regions (except the hippocampus) did not change significantly with the two administration regimens.

Bock et al. (16) reported saturation in SI enhancement starting from a cumulative dose of 180 mg/kg, administered in six injections of 30 mg/kg each (separated by 48 h). Apparently, we observed saturation in T_1 values at lower

cumulative dosages. However, clearance of Mn from the brain during the 7-day time interval may have played a role. Two animals belonging to the three-injection group were repeatedly imaged from day 8 to day 30. The half-time of Mn concentration was about 8 days, indicating that a substantial fraction of the Mn injected on day 1 would have cleared by the imaging time (day 8).

In conclusion, we have established a protocol based on fast T_1 mapping and coregistration of images to a rat brain atlas that allows absolute quantification of Mn concentration in brain regions. This protocol in principle could be used in functional experiments performed in awake animals.

ACKNOWLEDGMENTS

We thank A. Schwarz and A. Bifone (Glaxo-Smith-Kline Research Center, Verona, Italy) for kindly providing the T_2-weighted rat brain template, A. Lascialfari and M. Corti (University of Pavia, Pavia, Italy) for helpful discussions on the frequency dependence of brain relaxation rate, and M. Sandri for statistical analysis.

REFERENCES

1. Aoki I, Naruse S, Tanaka C. Manganese-enhanced magnetic resonance imaging (MEMRI) of brain activity and applications to early detection of brain ischemia. NMR Biomed 2004;17:569–580.
2. Silva AC, Lee JH, Aoki I, Koretsky AP. Manganese-enhanced magnetic resonance imaging (MEMRI): methodological and practical considerations. NMR Biomed 2004;17:532–543.
3. Aoki I, Tanaka C, Takegami T, Ebisu T, Umeda M, Fukunaga M, Fukuda K, Silva AC, Koretsky AP, Naruse S. Dynamic activity-induced manganese-dependent contrast magnetic resonance imaging (DAIM MRI). Magn Reson Med 2002;48:927–933.
4. Kuo Y, Herlihy AH, So P, Bell JD. Manganese-enhanced magnetic resonance imaging (MEMRI) without compromise of the blood-brain barrier detects hypothalamic neuronal activity in vivo. NMR Biomed 2006;19:1028–1034.
5. Yu X, Wadghiri YZ, Sanes DH, Turnbull DH. In vivo auditory brain mapping in mice with Mn-enhanced MRI. Nat Neurosci 2005;8:961–968.
6. Van der Linden A, Van Camp N, Ramos-Cabrer P, Hoehn M. Current status of functional MRI on small animals: application to physiology, pathophysiology, and cognition. NMR Biomed 2007;20:522–545.
7. Schwarz AJ, Danckaert A, Reese T, Gozzi A, Paxinos G, Watson C, Merlo-Pich EV, Bifone A. A stereotaxic MRI template set for the rat brain with tissue class distribution maps and co-registered anatomical atlas: application to pharmacological MRI. Neuroimage 2006;32:538–550.
8. Deichmann R, Haase A. Quantification of T_1 values by SNAPSHOT-FLASH NMR imaging. J Magn Reson 1992;96:608–612.
9. Paxinos G, Watson C. The rat brain in stereotaxic coordinates. 4th ed. San Diego: Academic Press; 1998.
10. Jenkinson M, Smith S. A global optimisation method for robust affine registration of brain images. Med Image Anal 2001;5:143–156.
11. Weaver BM, Staddon GE, Mapleson WW. Tissue/blood and tissue/water partition coefficients for propofol in sheep. Br J Anaesth 2001; 86:693–703.
12. Nordhøy W, Anthonsen HW, Bruvold M, Brurok H, Skarra S, Krane J, Jynge P. Intracellular manganese ions provide strong T_1 relaxation in rat myocardium. Magn Reson Med 2004;52:506–514.
13. Lee JH, Silva AC, Merkle H, Koretsky AP. Manganese-enhanced magnetic resonance imaging of mouse brain after systemic administration of $MnCl_2$: dose-dependent and temporal evolution of T_1 contrast. Magn Reson Med 2005;53:640–648.
14. Serrano F, Deshazer M, Smith KDB, Ananta JS, Wilson LJ, Pautler RG. Assessing transneuronal dysfunction utilizing manganese-enhanced MRI (MEMRI). Magn Reson Med 2008;60:169–175.
15. Yang J, Khong P, Wang Y, Chu AC, Ho S, Cheung P, Wu EX. Manganese-enhanced MRI detection of neurodegeneration in neonatal hypoxic-ischemic cerebral injury. Magn Reson Med 2008;59:1329–1339.
16. Bock NA, Paiva FF, Silva AC. Fractionated manganese-enhanced MRI. NMR Biomed 2008;21:473–478.
17. Silva AC, Bock NA. Manganese-enhanced MRI: an exceptional tool in translational neuroimaging. Schizophr Bull 2008;34:595–604.
18. Aime S, Anelli L, Botta M, Brocchetta M, Canton S, Fedeli F, Gianolio E, Terreno E. Relaxometric evaluation of novel manganese(II) complexes for application as contrast agents in magnetic resonance imaging. J Biol Inorg Chem 2002;7:58–67.
19. Cavagna FM, Marzola P, Daprà M, Maggioni F, Vicinanza E, Castelli PM, de Haën C, Luchinat C, Wendland MF, Saeed M, Higgins CB. Binding of gadobenate dimeglumine to proteins extravasated into interstitial space enhances conspicuity of reperfused infarcts. Invest Radiol 1994;29(Suppl 2):S50–S53.